Expression, purification and structural studies of a short antimicrobial peptide

Mateja Zorko, Boštjan Japelj, Iva Hafner-Bratkovič, Roman Jerala *,1

Department of Biotechnology, National Institute of Chemistry, Hajdrihova 19, POB 660, 1000 Ljubljana, Slovenia

A R T I C L E   I N F O

A B S T R A C T

We have produced a small antimicrobial peptide PFWRIRIRR in bacteria utilizing production in the form of insoluble fusion protein with ketosteroid isomerase. The recombinant peptide was rapidly and efficiently isolated by acidic cleavage of the fusion protein based on the acid labile Asp–Pro bond at the N-terminus of the peptide. The peptide has antibacterial activity and neutralizes macrophage activation by LPS. The selectivity of the peptide against bacteria correlates with preferential binding to acidic phospholipid vesicles. Solution structure of the peptide in SDS and DPC micelles was determined by NMR. The peptide adopts a well-defined structure, comprising a short helical segment. Cationic and hydrophobic clusters are segregated along the molecular axis of the short helix, which is positioned perpendicular to the membrane plane. The position of the helix is shifted in two micellar types and more nonpolar surface is exposed in anionic micelles. Overall structure explains the advantageous role of the N-terminal proline residue, which forms an integral part of the hydrophobic cluster.

© 2008 Elsevier B.V. All rights reserved.

1. Introduction

Treatment of bacterial infection with antibiotics is one of the mainstays of medicine [1]. Increasing resistance of virtually all microbes toward common antibiotics is a major health concern. Antimicrobial peptides are present in a variety of organisms where they protect the host from microbial infection. They have been identified in and isolated from a variety of sources including mammals, insects, amphibians, fish, plants, prokaryotes [2,3]. These peptides are less susceptible to the development of bacterial resistance because they act on the bacterial membrane causing multiple stress through several targets [4] but have minimal toxic and allergic effects to the host [5]. Thus, antimicrobial peptides may potentially be applied in medicine as safe antimicrobial agents due to their activities against bacteria and fungi [6]. Recent studies have shown that many cationic antimicrobial peptides are able to neutralize LPS [7], block cytokine induction in macrophages and prevent sepsis in animal models. Sepsis due to a Gram-negative bacteria is usually caused by the release of a bacterial outer membrane component, endotoxin (lipopolysaccharide, LPS) [7].

In order to provide large quantities of these peptides for physiological investigation and clinical trials, efficient production methods are necessary. Short antimicrobial peptides can be efficiently prepared by chemical synthesis, but may still be prohibitively expensive for therapy [8]. As an alternative, recombinant methods

permit the production of peptides and proteins in microorganisms. Production of antimicrobial peptides in expression systems, such as bacterial, yeast or insect cells has been reported. *Escherichia coli* has been used for production of many antimicrobial peptides, e.g. lactoferricin [9], dermicin [10], moricidin [11], defensins [12–14] and buforin [15]. This biological expression system is also suitable to obtain uniformly or partially isotopically enriched peptides, which are required for structural investigation of the ligand–receptor interaction by NMR spectroscopy and provides additional information on molecular dynamics, improvement of the precision of the determined structures and filtered experiments in the complex systems [16,17]. However, difficulties have been encountered in expression of antimicrobial peptides because of their cytotoxicity to host cells, sensitivity to proteolytic degradation and low expression level [18]. The expression system with an antimicrobial peptide fused to a partner protein is most effective because of the reduced toxicity against host cells, enhanced product stability and facilitated product recovery [19]. Such fusion proteins generally lack antimicrobial activity if they form insoluble products or interact with carrier protein [20–24]. The peptide is released from the fusion by chemical or enzymatic cleavage [25].

For this study we selected the peptide based on the structure–activity development of the peptide LF11 originating from human lactoferrin We have already reported solution structure of LF11 in complex with anionic and zwitterionic amphiphiles [16,26–28], where LF11 adopted a defined and unique fold in the micellar environment. We deleted most of the noncharged polar residues that do not contribute to the favorable interactions with anionic lipids or LPS and exchanged several residues, which increased its antimicrobial activity and neutralization of LPS. One of the key properties of antimicrobial

peptides is their ability to differentiate between foreign and host cells, which is defined but by the peptide structure and target membrane properties [29]. Importantly, eukaryotic and bacterial membranes have very different lipid compositions. The membrane of host cells comprises mainly phosphatidylcholine, sphingomyelin and cholesterol, whereas bacterial cells expose negatively charged phospholipids, phosphatidylglycerol, cardiolipin and lipopolysaccharides [30]. As demonstrated before, a high content of arginine and hydrophobic residues is essential for activity against bacterial membranes [31]. Short peptides are devoid of defined tertiary structure but can adopt a defined conformation in the lipid environment.

We have produced and purified a recombinant antimicrobial peptide PFWRIRIRR ("PFR peptide") using ketosteroid isomerase (KSI) as a fusion partner in *E. coli*. The fusion protein formed insoluble inclusion bodies in bacteria. We engineered a single Asp–Pro acid labile dipeptide between KSI and the PFR peptide, which allowed efficient production and isolation of the recombinant peptide in bacteria. We found that the peptide binds to the anionic but not to zwitterionic lipid vesicles and that the type of lipid mimetics significantly affects the peptide structure and may account for its antibacterial activity.

2. Materials and methods

2.1. Gene construct preparation

Oligonucleotide (5′-phosphate-GATCCGTTCTGGCGTATT CGCATCCGTCGCTGAATG-3′), the encoding peptide sequence, annealed with the corresponding complementary oligonucleotide, was ligated into pET31b (+) expression vector (Novagen) 3′ to the ketosteroid isomerase (KSI) gene using restriction site AlwN I [32].

2.2. Media and culture conditions

For protein expression, the *E. coli* BL21 (DE3) pLysS (Invitrogen) transformed with pET31b(+) encoding KSI–PFR gene and was grown in TB medium. Fermentation was performed in shake flasks with 100 µg/ml ampicillin at 37 °C and 220 rpm. Measuring the optical density at 600 nm monitored cell growth. When cultures reached an OD_{600} of 0.8, IPTG at 0.4 mM final concentration was added to the culture broth for induction of the production of recombinant KSI–PFR protein. Four hours after induction, bacteria were harvested by centrifugation at 700 rpm for10 min.

2.3. Purification of the expressed proteins

To purify the recombinant proteins, the cell pellet was suspended in the lysis buffer (10 mM Tris pH 8.0, 1 mM EDTA, 0.1% DOC) and lysed by sonication. The bacterial lysate was centrifuged at 12000 rpm for 15 min at 4 °C to separate the soluble supernatant and insoluble pellet fraction containing inclusion bodies. The insoluble inclusion body fraction containing KSI–PFR fusion proteins was washed with a series of wash buffers (10 mM Tris pH=8.0, 1 mM EDTA, 0.1% DOC, twice; 10 mM Tris pH=8.0, 1 mM EDTA, 0.1% DOC, 2 M urea, twice and with 20 mM Tris pH=8.0 three times). After every wash the mixture was centrifuged at 12,000 rpm for 10 min at 4 °C. The insoluble inclusion bodies were dissolved in 6 M guanidine–HCl and centrifuged. Soluble supernatant dialyzed against deionized water that caused precipitation of KSI–PFR. Fusion proteins were resuspended in 90 mM HCl, the suspension was mixed for 2 h at 85 °C to cleave the aspartyl–prolyl bond between the KSI segment and recombinant peptide. The peptide was purified by HPLC on a C5 RP-HPLC column (Supelco) using a gradient of 5% acetonitrile, 5 mM HCl and 95% acetonitrile and 5 mM HCl and freeze dried using repeated washes with water. The peptide peak was detected by UV absorbance at 280 nm. The identity of the peptide peak was determined by mass spectrometry.

2.4. Peptide synthesis

The PFR peptide was chemically synthesized by KECK center (Yale University, New Haven, CT, USA) using Fmoc chemistry. The purity of the synthetic peptide was determined by HPLC and MS analysis.

2.5. Assay of antimicrobial activity

The antibacterial activity of the purified recombinant PFR was compared to that of the synthetic peptide, using *E. coli* (NCTC 8007, serotype 0111 K58 H2) that was provided by Prof. Ignacio Moriyon, University of Navarra Pamplona, Spain. Bacterial cultures were stored at −80 °C and grown on minimal medium at 37 °C. Antimicrobial activity was determined using standard microbroth dilution assay in minimal medium.

2.6. Inhibition of NO production in LPS-stimulated RAW264.7 macrophages

The RAW264.7 macrophage cell line was cultured in RPMI supplemented with antibiotic (penicillin 100 IU/ml and streptomycin 100 µg/ml; Gibco) and 12% fetal bovine serum (Perbio) at 37 °C under 5% CO_2. The cell suspension of 1 million cells/well and 100 µM carboxy-PTIO (Sigma) was treated with either LPS (100 ng/ml) alone or with various concentrations of PFR (10–100 µg/ml) for 24 h. Nitric oxide was measured as its end product using Griess reagent (Sigma). The 100 µl culture supernatant from the culture of RAW264.7 cells was mixed with an equal volume of Griess reagent and the absorbance was measured at 570 nm [33].

### 2.7. Preparation of unilamellar vesicles

Large unilamellar lipid vesicles (LUVs) used for ITC and fluorescence experiments were prepared by extrusion method using a Mini-Extruder (Avanti Polar lipids Inc.). The multilamellar vesicle suspension was freeze–thawed for 5 cycles and then extruded 10 times through polycarbonate filters (0.1 µm).

2.8. Fluorescence spectroscopy

Tryptophan fluorescence was measured using a Perkin-Elmer LS 55 luminescence spectrometer. Either 1 mM POPG or 1 mM POPC was introduced to 12 µM peptide in PBS. The excitation wavelength used was 295 nm and the emission scanned from 300–450 nm with a scan speed of 300 nm/s. Fluorescence quenching experiments were performed by stepwise addition of acrylamide from stock solution of 1 M into peptide containing solutions in the absence or presence of vesicles at peptide/lipid molar ratio 1:140. Emission spectra, as previously described, were collected after each addition of quencher up to the final acrylamide concentration of 0.5 M. The data were analyzed according to the Stern–Volmer equation, $F_0/F = 1 + K_{SV} [Q]$, where F_0 and F are the fluorescence intensities in the absence and the presence of the quencher (Q) and K_{SV} is the Stern–Volmer quenching constant, providing a measure for the accessibility of Trp to acrylamide.

2.9. Determination of haemolytic activity

Heparin (4 µl at 5000 IU/ml) was added to 100 µl of fresh peripheral blood from a healthy volunteer and centrifuged at 2000 rpm for 10 min at room temperature. We washed the pellet of red blood cells with phosphate-buffered saline (PBS) and prepared a 2% (vol/vol) suspension of erythrocytes in PBS. Fifty microliters of the peptide in the concentration range from 10^{-6} to 10^{-4} M in PBS and 50 µl of erythrocyte suspension were incubated at 37 °C for 1 h. For a positive control, we used 2% (vol/vol) Triton X-100 in PBS, which caused 100% hemolysis. After the incubation, samples were centrifuged for 5 min at 2200 rpm at room temperature, and absorbance at 405 nm was measured.
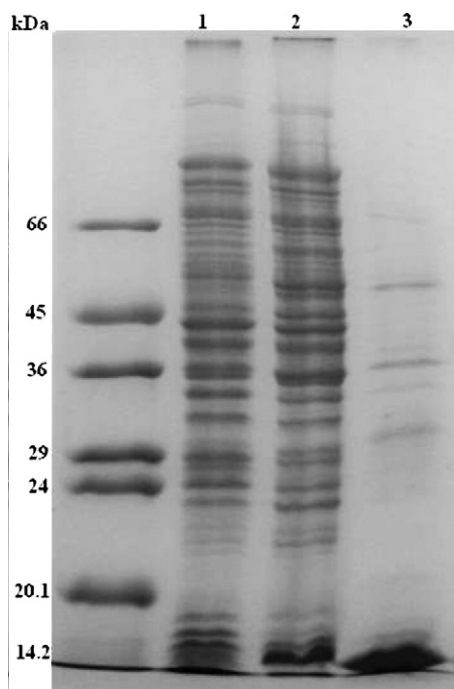
Fig. 1. SDS-PAGE analysis of protein production in bacteria. Lanes 1 and 2 represent total bacterial lysate of non-induced bacteria (1) and bacteria 4 h after IPTG induction (2). Lane 3 represents inclusion bodies after purification. Proteins were stained with Coomassie brilliant blue.

2.10. Isothermal titration calorimetry

ITC data were acquired using a VP-ITC calorimeter (Microcal, LLC). Samples were prepared with 20 μM peptide and either 5 mM POPG or POPC in 10 mM Tris pH 7 and 100 mM NaCl. To account for the heat of dilution titrating the lipid vesicles into a buffered solution in the absence of peptide completed the control experiments. All experiments were carried out at 20 °C. Titration was carried out over a 170 min period, with 300 s between individual 5 μl injections.

2.11. Nuclear magnetic resonance (NMR) spectroscopy

PFR in SDS sample was prepared by dissolving 1.2 mg of the peptide in 500 μl of sodium phosphate buffer which contained 232 mM D_{25}-sodium-dodecylsulphate and 8% D_2O. The pH was adjusted to 5.5. PFR peptide in DPC was prepared by dissolving 1.1 mg of the peptide in 460 μl of sodium phosphate buffer that contained 200 mM of D_{38}-dodecylphosphocholine. 40 μl of D_2O was added to the sample and pH was adjusted to 5.1. The final peptide concentration was 1.8 mM. A sample of ^{15}N-labeled recombinant PFR in SDS was prepared by dissolving 0.4 mg of PFR in 300 μl of sodium phosphate buffer solution, which contained 127 mM d25-SDS and 8% D_2O. Spectra were recorded at 30 °C on a Varian Unity INOVA 600 MHz spectrometer equipped with 5 mm $^1H(^{13}C/^{15}N)$ Pulse Field Z-Gradient Triple Probe. 2-D homonuclear TOCSY and NOESY spectra were acquired using WET [34] or WATERGATE [35] suppression scheme. TOCSY spectra were recorded at mixing times of 10 and 80 ms. NOESY spectra were recorded at mixing times of 80 and 150 ms. 2048×256 data points and spectral widths of 8000 Hz in both dimensions were used with 48 to 128 transients. The HSQC spectrum was acquired with 2048×256 data points. WURST80 decoupling was used to remove coupling from NH protons. Spectra were assigned using Felix (Acclerys) software. Calibration of volumes and conversion of volumes into DYANA restraints for upper bounds was achieved using nmr2st program [36]. Two well resolved aromatic proton crosspeaks of I5: HG11-I5: HG12 and I7: HG11-I7: HG12 were

used for calibration. The experimental distance constraints were then employed to generate peptide conformers using 6000 steps of simulated annealing in torsion angle space implemented in the program DYANA version 1.5 [37]. 20 structures with the lowest target function out of 100 calculated structures were kept for further minimization. Program DISCOVER (Accelrys) using the cvff force field (21) was used to energy minimize the structures. The quality of structures was checked with PROCHECK_NMR [38]. Structures were visualized and analyzed with MOLMOL [39].

3. Results

### 3.1. Production of recombinant antimicrobial peptide in bacteria

Short peptides can be overexpressed in bacteria in the form of fusion proteins, where both bacteria and peptide are protected from membranolytic and proteolytic activity, respectively. The peptide is usually released from the fusion protein by chemical cleavage using CNBr or hydroxylamine, which can however due to their reactivity cause formation of unwanted side products [40–43]. Therefore we have designed a fusion protein of a PFR peptide with ketosteroid isomerase (KSI–PFR) where we have utilized the acid sensitivity of the Asp–Pro bond engineered at the N-terminus of the peptide. This bond is cleaved in diluted acid at rates at least 100 times more efficient than other peptide bonds. Selective hydrolysis of aspartyl bonds involves intramolecular catalysis by aspartic carboxylate attack of the subsequent carbonyl group with simultaneous donation of a proton to the peptide bond nitrogen and consequent anhydride formation resulting in peptide bond cleavage [40–43]. The recombinant fusion protein was expressed in high yield in *E. coli* and accumulated in the form of inclusion bodies. Approximately 550 mg of pure recombinant protein was obtained from 1 l of culture medium. On SDS-PAGE this is seen as a band around the molecular weight of 14 kDa, as expected for the recombinant protein KSI–PFR (Fig. 1).

3.2. Cleavage of the fusion protein at acidic pH

Different conditions were examined to cleave the bond between the fusion protein and recombinant peptide. Fusion protein was treated with 60 to 90 mM HCl for various times to cleave the Asp–Pro bond between the KSI carrier protein and peptide. Alternatively, protein was dissolved in guanidine–HCl acidified by formic acid. The highest amount of the peptide was produced by treatment with
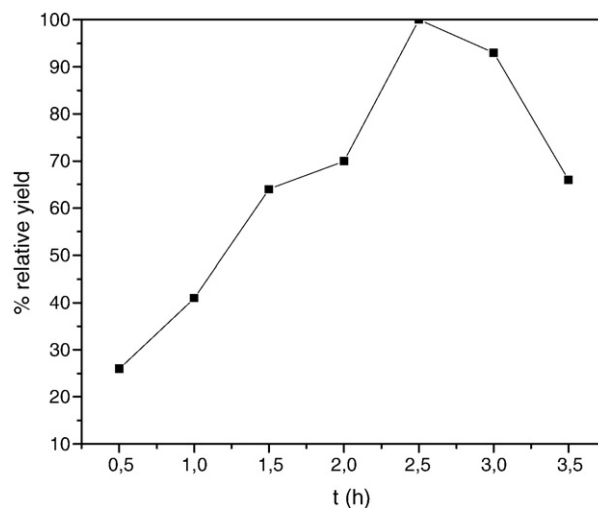
Fig. 2. Time dependence of peptide cleavage from fusion protein. The fusion protein KSI–PFR was suspended in diluted acid (90 mM HCl) and mixed at 85 °C to cleave the aspartyl–prolyl bond between the fusion protein and peptide.
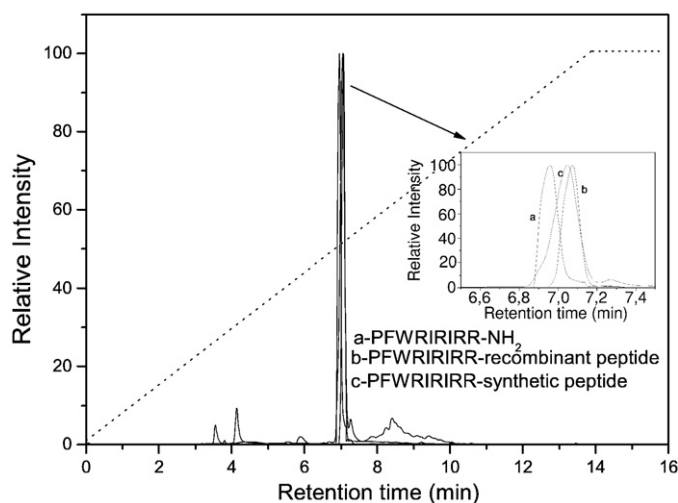
Fig. 3. Reverse-phase HPLC purification of recombinant PFR peptide after cleavage of the KSI–PFR. Peak eluting at 7 min represents the purified peptide. Magnified inset shows the difference in elution between synthetic amidated PFR peptide (a) and synthetic and recombinant PFR (b), which elute at identical retention time. Peptide was eluted by a gradient from 0 to 95% acetonitrile and 5 mM HCl within15 min.

90 mM HCl at 85 °C for 2.5 h and decreased afterwards (Fig. 2). The final yield was 10 mg of purified peptide from 550 mg of recombinant protein per liter of bacterial culture. Following the cleavage, the reaction mixture was purified by HPLC (Fig. 3). As can be seen, most of the KSI remained insoluble and the peptide represented more than 80% of the material eluted from the column. Mass spectroscopy was used to verify the identity of the purified peptide and its labeling in ^{15}N isotopically enriched minimal medium (Fig. 4). Polypeptide backbone of the isotopically labeled peptide has been assigned (data not shown) and will be used to measure interaction of peptide with bacteria and investigate dynamic properties of the peptide.

3.3. Biological activity of the peptide

Antimicrobial activity of peptide was examined against *E. coli.* All tested peptide variants inhibited bacterial growth. The minimal inhibitory concentration for the recombinant peptide was 18 ± 2 µg/ml in comparison to 6 ± 3 µg/ml and 48 ± 3 µg/ml for the amidated and nonamidated synthetic peptide, respectively. Amidation increased the net charge of the peptide and its affinity to anionic lipids, which is probably the reason for higher antimicrobial activity of amidated
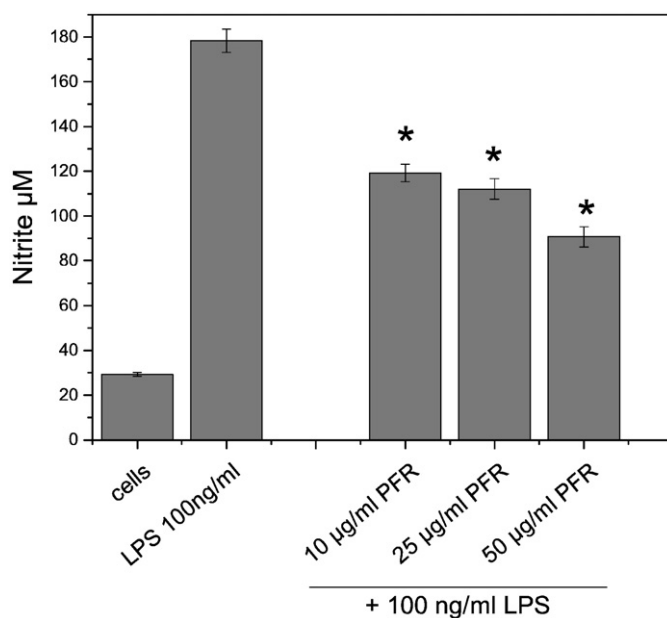

Fig. 5. Recombinant PFR peptide inhibits LPS stimulated NO production by murine macrophages. Macrophages were stimulated with 100 ng/ml of LPS in the presence of varying peptide concentrations and nitrite was determined in the supernatants using Griess reaction. Data points represent standard errors of the means of the results obtained from three experiments. The asterisks indicate a significant decrease in nitrite level compared to the results obtained with cells treated with LPS only ($P < 0.05$).

peptide. However despite using the same purification procedure and the same MS spectra (Figs. 3 and 4) recombinant peptide was consistently more active than synthetic peptide, probably because of some contaminant from the synthesis although the precise reason could not be determined. Neither recombinant nor synthetic peptides were hemolytic to human erythrocytes up to concentration of 500 µg/ml. Peptides based on human lactoferrin have previously shown neutralization of bacterial endotoxin, which prevents the cellular activation of macrophages by LPS. To determine the inhibitory effect of the peptide on nitric oxide production in LPS stimulated macrophages, cells were treated with LPS and different concentrations of recombinant peptide. NO production was assayed by measuring nitrite (a stable degradation product of NO) in the supernatant of cultured RAW264.7 cells. Recombinant peptide did not activate the cells, which indicates the absence of LPS contamination and was able to inhibit cell activation by LPS (Fig. 5).
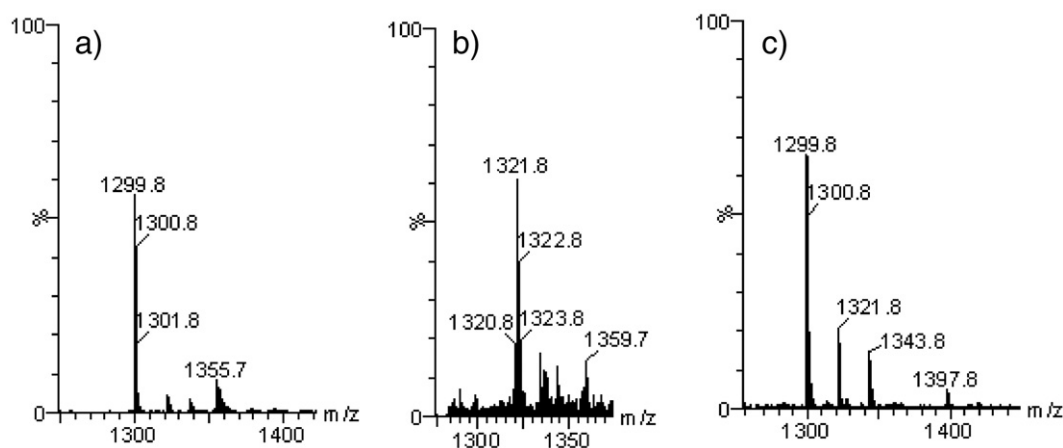
Fig. 4. Mass spectroscopic analysis of the recombinant peptide prepared in bacteria (a), ^{15}N uniformly enriched recombinant peptide (b) and synthetic peptide (c). Theoretical molecular weight of peptides is 1299.5 (a), 1321.5 (b) and 1299.5 (c).
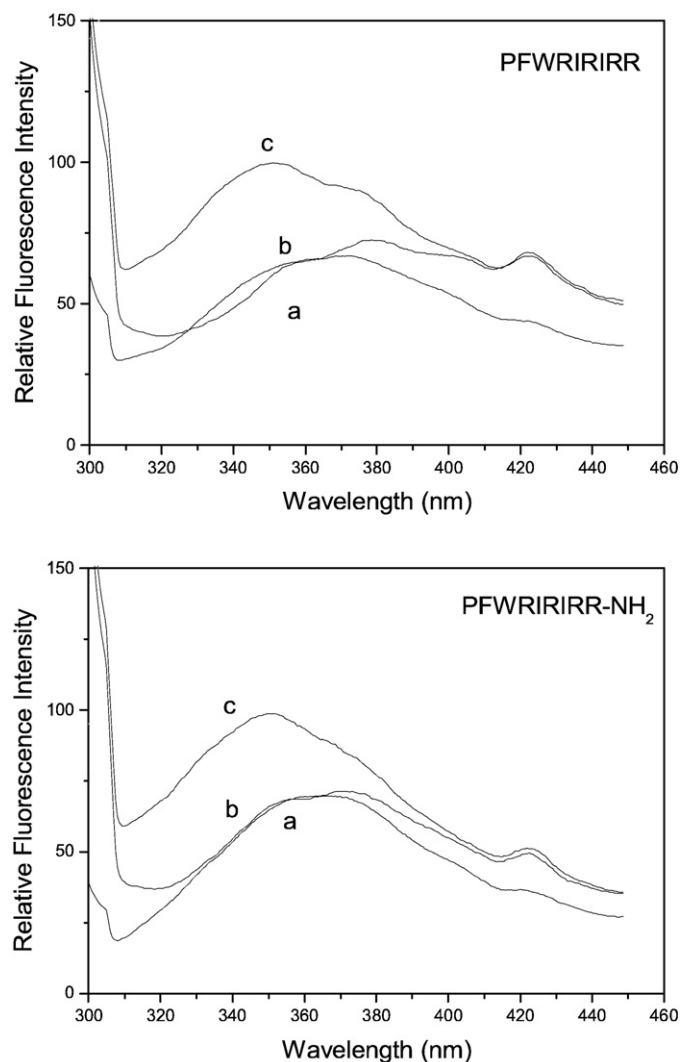
Fig. 6. Differences in synthetic PFR peptide (top, PFR and bottom, amidated PFR peptide) interaction with anionic and zwitterionic phospholipid vesicles determined by intrinsic tryptophan fluorescence. Fluorescence emission spectra of 12 μM PFR in PBS buffer were determined in (a) buffer only, (b) 1 mM POPC and (c) 1 mM POPG.

3.4. Peptide interaction with lipid vesicles

Negatively charged POPG vesicles were used to mimic bacterial membranes and zwitterionic POPC as eukaryotic membrane mimetics. The fluorescence emission spectra of PFR in the presence of POPG and POPC are shown in Fig. 6. Binding of the peptide to vesicles caused 15 nm blue shift in the emission maximum for POPG vesicles, while the emission maximum of the peptide in the presence of POPC vesicles remained essentially unchanged. Blueshift in the presence of POPG was accompanied by an increase in the fluorescence intensity, consistent with partitioning of the Trp side chain into a more hydrophobic environment [44]. Both amidated and nonamidated peptide displayed a similar effect of different membrane mimetics.

3.5. Fluorescence quenching of intrinsic peptide fluorescence in different types of environment

In order to investigate the extent of the exposure of tryptophan residue to the solvent, a fluorescence-quenching study was performed using a neutral quencher acrylamide. In the presence of acrylamide the Trp fluorescence emission of the synthetic PFR peptide in an aqueous buffer decreased in a concentration dependant manner,

yielding a Stern–Volmer constant of 28.4 M^{-1} (Fig. 7). In the presence of POPC the K_{SV} decreased to 18.1 M^{-1} and further to 6.3 M^{-1} for POPG vesicles. A lower K_{SV} indicates a greater degree of protection of the Trp residue and indicates that the fluorophore is inserted into the hydrophobic core of the bilayer. In the case of POPC liposomes the Trp residue was more accessible to the quencher indicating weaker interaction and membrane insertion into the membrane. Amidated peptide however showed an increased degree of protection also in the presence of POPC micelles, which indicates deeper burial of the tryptophan residue within the lipid layer. Described results therefore indicate three different types of environment of the peptide tryptophan residue: it is protected against quenching in both types of lipids (more so in POPG), while as opposed to POPC the Trp side chain is in a more apolar environment in POPG. A likely explanation is that tryptophan inserts into the hydrophobic core of POPG vesicles while burial in case of POPC requires the presence of C-terminal amidation, whereas in case of nonamidated peptide it may only associate with surface headgroup region of POPC vesicles.

3.6. Isothermal calorimetric titration of peptide with phospholipid vesicles

The use of ITC provided an opportunity to determine whether the difference in interactions between neutral and negative lipids would be detectable and reflected by isothermal titration calorimetry [44].
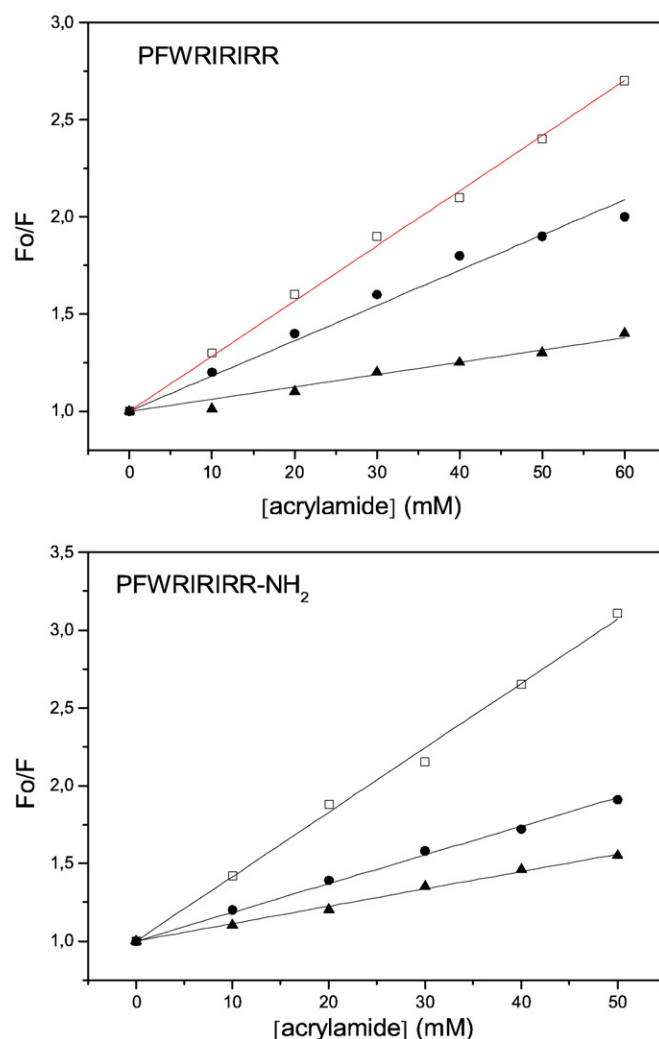
Fig. 7. Stern–Volmer plots for the quenching of Trp fluorescence emission of synthetic PFR peptide (top) and synthetic amidated PFR peptide (bottom) by acrylamide in a buffer (□) and in the presence of liposomes composed of POPC (●) and POPG (▲).
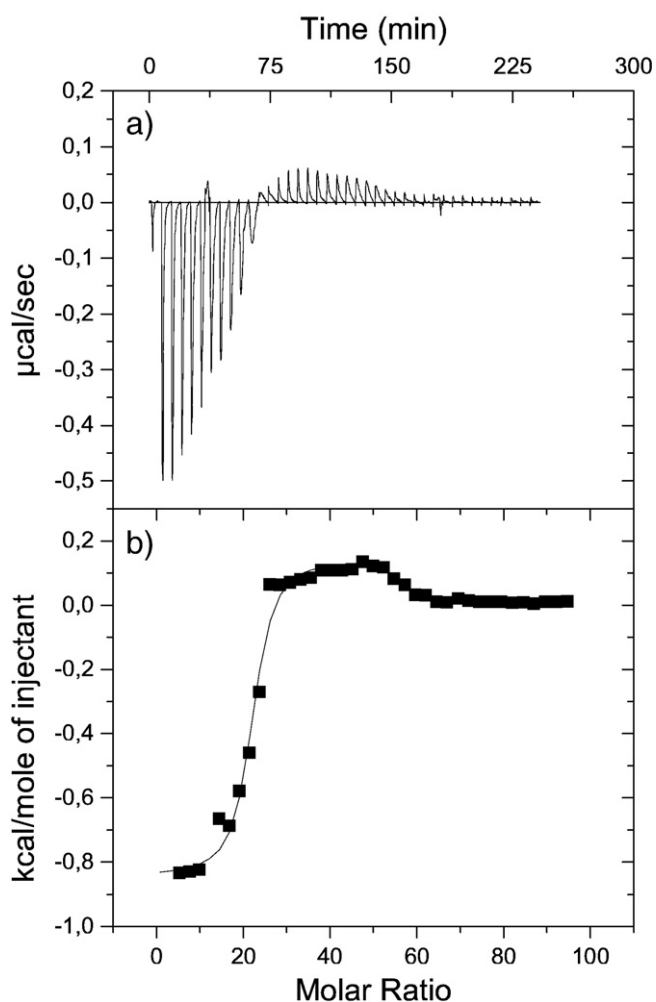
Fig. 8. Binding of synthetic PFR peptide to POPG vesicles determined by isothermal calorimetry. (a) A representative liposome titration assay obtained for PFR peptide (20 μM) titrated with 5 μl of 5 mM POPG in 10 mM Tris pH 7 and 100 mM NaCl. (b) The enthalpy changes for each titration data point.

The enthalpy of binding was studied by titration of either POPG or POPC vesicles into the peptide solution. The result of the interaction of the peptide to POPC indicated that the energy change was below the

sensitivity limit of the technique (data not shown). Binding of the peptide to POPG is shown in Fig. 8. The binding enthalpy indicates that peptide interaction with POPG vesicles is an exothermic process. Best fit was obtained with two binding site equation yielding $K1 = 4.7 * 10 + 7$ in $K2 = 4.1 * 10 + 5$ M−1. Reaction stoichiometry was estimated at a lipid to peptide ratio of 21 and 36 for the first and second step. First step indicates a significant entropic contribution, probably due to the penetration of the peptide into the hydrophobic core of the membrane. Isothermal titration of peptide to lipids has been observed before and has been attributed to membrane processes such as pore formation or membrane disruption have been proposed [45], although it could also be due to the formation of the second layer of bound peptide at higher peptide:lipid ratios.

### 3.7. Structure of peptide in micellar environment

3.7.1. Structure of PFR peptide in SDS micelles

NMR crosspeak assignments of the most active, synthetic amidated PFR peptide were made using a combination of 2D-TOCSY and 2D-NOESY spectra. Most crosspeaks were resolved in the fingerprint region of the NOESY spectrum except an overlap between Arg^8 and Arg^9 H^N–H^α resonances. H^N chemical shifts were in the range between 7.46 and 8.44 ppm. The chemical shift of Phe^2 H^α and H^N resonances were 4.69 and 8.44. Only 2D NOESY spectra were determined for recombinant PFR in SDS and showed high similarity with amidated synthetic peptide. Secondary chemical shift, $\Delta\delta$, was calculated for H^α atoms as the difference between the random coil chemical shift, δ_{RC}, and the measured chemical shift $\delta_{measured}$ [46]. Secondary chemical shifts of the H^α resonances contain the information on the secondary structure of peptides or proteins. An upfield (positive) shift is characteristic for an α-helix, whereas a downfield (negative) shift is characteristic for a β-conformation [47] (Fig. 9). Secondary chemical shift values indicate the presence of α-helical segments in both SDS and DPC micelles. The helical region lies at the N-terminus in DPC, while it is shifted towards the region between W3–R6 in SDS.

The solution structure of PFR in SDS was calculated based on 103 distance constraints. The backbone conformation of the peptide forms a short α-helical turn between residues Trp^3 and Arg^6 (Fig. 10) in agreement with secondary chemical shift values. PFR conformation in SDS micelles is well-defined, with backbone r.m.s.d. of 0.15 Å for the residues 2–8. The heavy atom r.m.s.d. of hydrophobic residues (Pro^1, Phe^2, Trp^3, Ile^5, Ile^7) is only 0.60 Å in comparison to the overall r.m.s.d. of 1.33 Å. Pro^1, Phe^2 and Trp^3 are clustered together with the side chain of the N-terminal proline between two aromatic residues. Three N-
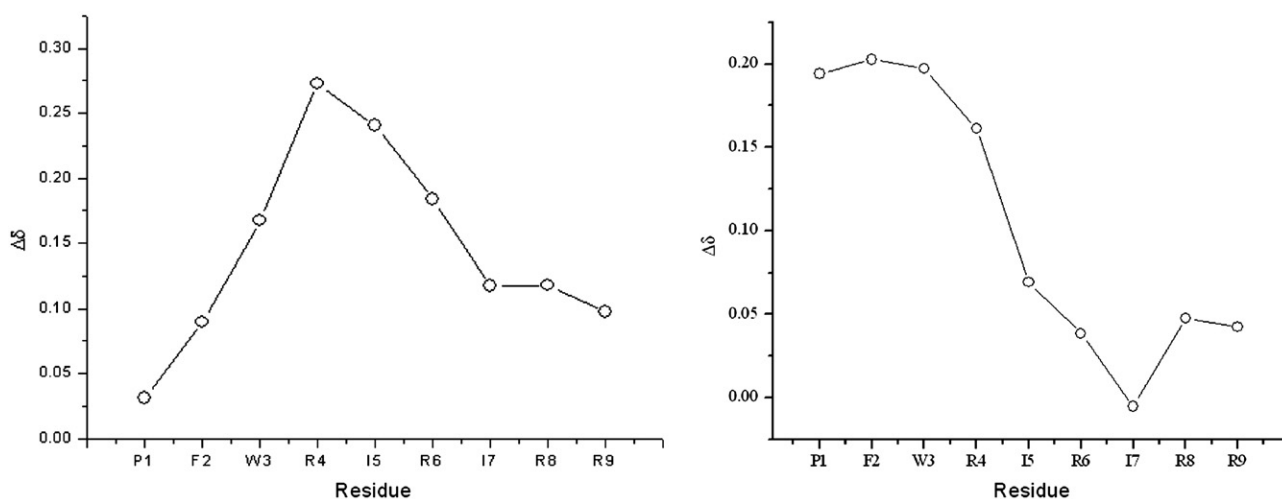
Fig. 9. Secondary chemical shifts for H^α protons of synthetic PFR peptide in SDS micelles (left) and in DPC micelles [61] calculated as an average value of H chemical shifts of three consecutive residues.
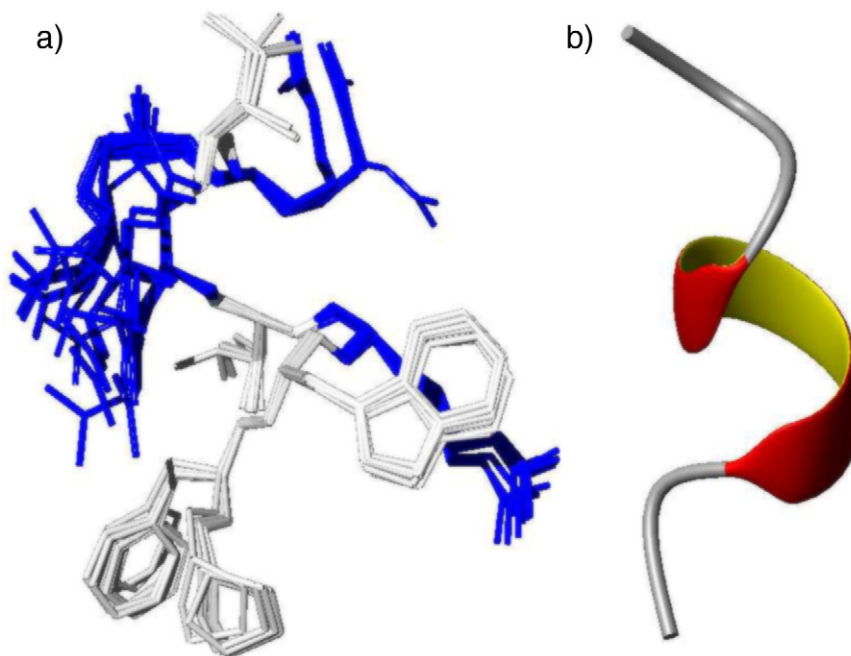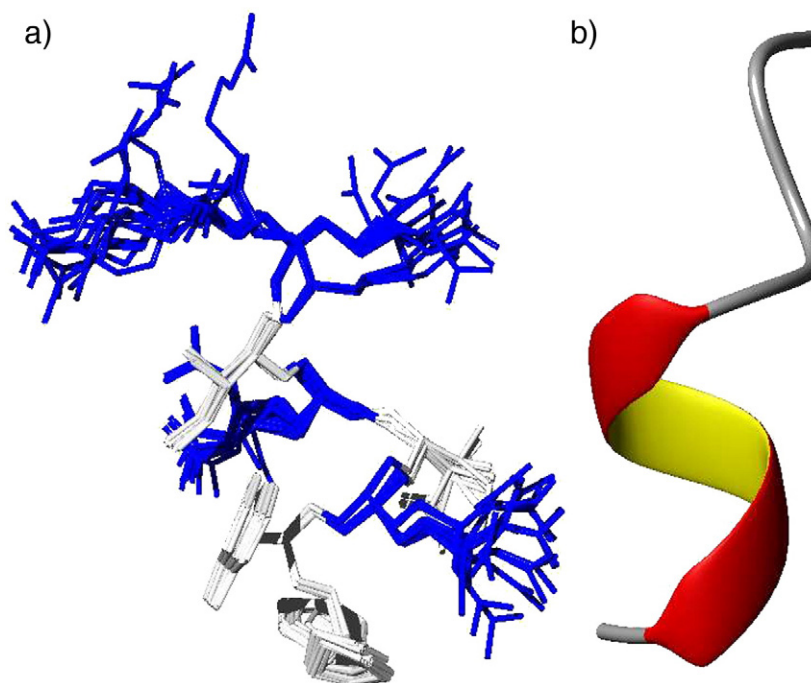
Fig. 10. (a) Solution structure of synthetic amidated PFR in SDS micelles, represented by an ensemble of 20 structures. (b) Backbone conformation of the representative structure of PFR in complex with SDS. Cationic residues are represented with blue lines.

terminal residues form a large hydrophobic surface with large lateral dimension and may thus be able to induce defects when inserted into the bacterial membrane. Arg^4 forms the energetically favorable cation-π interaction with the aromatic group of Trp3, which could facilitate deeper embedding of PFR into anionic membranes. The side chains of Arg^6, Arg^8 and Arg^9 are positioned around the axis of the short helical segment and point to different directions.

3.7.2. Structure of PFR peptide in DPC micelles

The structure of PFR in the presence of DPC micelles was calculated using 79 distance constraints. PFR structure in DPC is also well defined with a backbone r.m.s.d of 0.38 Å. The backbone also forms one turn of α-helix, which is however in comparison to the SDS structure shifted towards the N-terminus and positioned between residues Phe^2 and Ile^5 (Fig. 11). The heavy atom r.m.s.d. of

Fig. 11. (a) Solution structure of synthetic amidated PFR in DPC micelles, represented by an ensemble of 20 structures. (b) Backbone conformation of the representative structure of PFR in complex with DPC. Cationic residues are represented with blue lines.

Table 1

Structural statistics of PFR ensemble	SDS	DPC
Distance restraints		
Total NOE	97	79
Intraresidual	34	37
Sequential ($|i–j|$=1)	40	24
Non-sequential ($|i–j|$>1)	23	18
Structure statistics		
Min and max. violations (Å)	0.65, 0.98	0.36, 0.78
Backbone atoms (residues 2–7)	0.15±0.05	0.38±0.29
Heavy atoms (residues 2–7)	1.37±0.37	1.30±0.26
Ramachandran plot quality		
Residues in the most favored regions (%)	67.9	53.6
Residues in additional allowed regions (%)	32.1	44.3
Residues in generously allowed regions (%)	0.0	2.1
Residues in disallowed regions (%)	0.0	0.0

Peptide structures were deposited at BioMagResbank under the codes 20012 and 20013 for the structure in SDS and DPC, respectively.

hydrophobic residues is 0.68 Å in comparison to overall r.m.s.d. of 1.26 Å. Ile5 lies close to Phe2, Arg[4] and Arg[6] are located close to the hydrophobic core of the peptide and available for electrostatic interactions with the phosphate group of micelles, whereas Arg[8] and Arg[9] in the C-terminal part of the peptide are oriented away from the hydrophobic core. In contrast to the SDS structure there is no energetically favorable Trp–Arg interaction, which has been shown to stabilize the peptide fold in membranes [48].

The comparison between the structure of PFR in SDS and DPC shows that the peptide is in an α-helical conformation between residues 3 and 6 in complex with SDS micelles and between residues 2 and 5 in complex with DPC. The main difference is in the N-terminal hydrophobic segment. Trp[3] in the DPC structure is oriented towards the Ile[7], and Ile[5] closer to Phe[2], which makes it more compact. This is evident from the higher solvent exposed surface of the structure in SDS (1514 vs.1464 Å[2]), which is mainly due to the increased nonpolar surface (704 vs. 653 Å[2]) (Table 1).

4. Discussion

Peptides are in comparison to most antimicrobials still relatively expensive to produce, which is one of the reasons hindering their application. The high cost of synthetic peptide synthesis and low yield of isolation from the natural host stimulates exploration of recombinant production of antimicrobial peptides [22,25,32,49–51]. In our study we used KSI as a partner protein that is expressed as an insoluble protein and accumulates in form of inclusion bodies. Most reported antimicrobial peptides were longer than 20 residues, however even recombinant production of a 9-residue peptide resulted in a high yield even without any particular optimization of bacterial fermentation. Normally, fusion proteins are produced in the form of inclusion bodies that can be efficiently solubilized and recombinant

fusion proteins are chemically or enzymatically cleaved to release the desired antimicrobial peptide product. Protease cleaves with low efficiency on insoluble protein aggregates, and thus researchers have sought to establish a useful chemical strategy. Previous studies have reported the release of antimicrobial peptides from fusion partners by digestion with CNBr, which can cleave peptides at methionine residues and hydroxylamine which can cleave Asn–Gly peptide linkages [19]. In our system diluted HCl liberated the peptide from the fusion protein at high yield and simplified the isolation procedure. The recombinant peptide consistently exhibited slightly better antimicrobial and endotoxin-neutralizing activity as the synthetic peptide and was indistinguishable by analytical techniques (MS and HPLC), nevertheless additional amidation of the synthetic peptide improved the antimicrobial activity due to the increased affinity for anionic lipids. It has been shown previously that the presence of additional charge may significantly affect the membrane interacting and biological properties of peptides [52–54]. The selected strategy requires the N-terminal proline residue of the peptide, which is in fact even favorable for the selected peptide. We have shown the essential structural role of the proline residue for the peptide conformation adopted in the membrane mimetic environment. PFR interacts preferentially with negatively charged membranes, which provides its selectivity and high therapeutic index.

The structure of the PFR peptide in SDS and DPC was determined and in both types of micelles the peptide forms a well-defined conformation. The peptide in complex with SDS contains α-helical conformation between residues 3 and 6 and between residues 2 and 5 in complex with DPC. In contrast to most amphipathic α-helical antimicrobial peptides [55] the amphipathic moment lies along the helical axis and not perpendicular to it (Fig. 12). This can only be accomplished because of the small size of the peptide. Clusters of hydrophobic residues are essential for antimicrobial activity [56], however a high amount of tryptophan residues increases the nonspecific binding to eukaryotic membrane and hemolytic activity [57,58]. The PFR peptide contains only a single tryptophan residue and an additional phenylalanine residue, which is responsible for its high specificity for anionic membranes and the absence of haemolytic activity. Alternating Arg–Ile residues in the region 4 to 8 induce formation of a short helical segment in the peptide. Three hydrophobic residues at the N-terminus of the PFR peptide form a cluster, which is more compact in the zwitterionic environment and has a larger lateral dimension in anionic micelles. The difference in the charge distribution of PFR in anionic and zwitterionic micelles as well as arrangement of hydrophobic side chains contributes to the mechanism of selective discrimination between bacterial and eukaryotic membranes. This structural difference is most likely due to the electrostatic interaction between cationic residues closest to the membrane surface (Arg[4] and Arg[6]) with negatively charged surface head groups of anionic vesicles which embeds the peptide deeper into the micelle, disrupts the interaction of Trp[3] with Ile[7] and causes dislocation of the helix. Interaction of guanidinium groups on
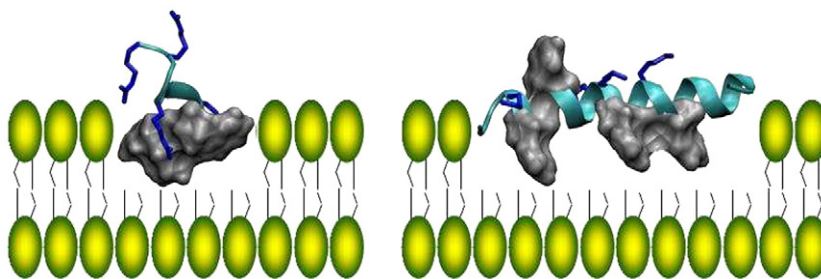
Fig. 12. Schematic representation of the orientation of PFR peptide inserted into the membrane (left) and typical α-helical peptide (magainin, right). PFR peptide α-helical axis lies perpendicular to the membrane plane, while for longer α-helix of magainin it is parallel to the plane of the membrane. Side chains of cationic residues are shown as blue sticks as hydrophobic residues as surface representation.

arginine residues with phosphate groups of phospholipids has been determined before for PG-1 by solid state NMR and proposed to contribute to the formation of membrane defects [59]. N-terminal proline, which was introduced because of the recombinant peptide production approach was essential for the integrity of the structure and improved the antimicrobial activity. Proline forms an essential part of the hydrophobic cluster, with many side chain contacts with side chains of Phe^2 or Trp^3. The N-terminal hydrophobic cluster of the PFR peptide has similar function as the short acyl chain of the lipopeptide [60]. The structures in this report can be used to improve the design of more selective peptides by enhancing the differences in local conformational changes caused in zwitterionic and anionic membranes.

Acknowledgements

References

[1] K.A. Brogden, Antimicrobial peptides: pore formers or metabolic inhibitors in bacteria? Nat. Rev., Microbiol. 3 (2005) 238–250.

[2] H.G. Boman, Peptide antibiotics and their role in innate immunity, Annu. Rev. Immunol. 13 (1995) 61–92.

[3] R.E.W. Hancock, R. Lehrer, Cationic peptides: a new source of antibiotics, Trends Biotechnol. 16 (1998) 82–88.

[4] U. Pag, M. Oedenkoven, V. Sass, Y. Shai, O. Shamova, N. Antcheva, A. Tossi, H.G. Sahl, Analysis of in vitro activities and modes of action of synthetic antimicrobial peptides derived from an alpha-helical 'sequence template', J. Antimicrob. Chemother. 61 (2008) 341–352.

[5] R.I. Lehrer, A.K. Lichtenstein, T. Ganz, Defensins — antimicrobial and cytotoxic peptides of mammalian-cells, Annu. Rev. Immunol. 11 (1993) 105–128.

[6] K. Hilpert, R. Volkmer-Engert, T. Walter, R.E.W. Hancock, High-throughput generation of small antibacterial peptides with improved activity, Nat. Biotechnol. 23 (2005) 1008–1012.

[7] Y. Rosenfeld, N. Papo, Y. Shai, Endotoxin (lipopolysaccharide) neutralization by innate immunity host-defense peptides — peptide properties and plausible modes of action, J. Biol. Chem. 281 (2006) 1636–1643.

[8] C.B. Park, H.S. Kim, S.C. Kim, Mechanism of action of the antimicrobial peptide buforin II: buforin II kills microorganisms by penetrating the cell membrane and inhibiting cellular functions, Biochem. Biophys. Res. Commun. 244 (1998) 253–257.

[9] H.K. Kim, D.S. Chun, J.S. Kim, C.H. Yun, J.H. Lee, S.K. Hong, D.K. Kang, Expression of the cationic antimicrobial peptide lactoferricin fused with the anionic peptide in *Escherichia coli*, Appl. Microbiol. Biotechnol. 72 (2006) 330–338.

[10] I. Cipakova, J. Gasperik, E. Hostinova, Expression and purification of human antimicrobial peptide, dermcidin, in *Escherichia coli*, Protein Expression Purif. 45 (2006) 269–274.

[11] S. Hara, M. Yamakawa, Production in *Escherichia coli* of moricin, a novel type antibacterial peptide from the silkworm, *Bombyx mori* (vol 220, pg 664, 1996), Biochem. Biophys. Res. Commun. 224 (1996) 877–878.

[12] I. Cipakova, E. Hostinova, J.G. Gasperik, V. Velebny, High-level expression and purification of a recombinant hBD-1 fused to LMM protein in *Escherichia coli*, Protein Expression Purif. 37 (2004) 207–212.

[13] Z.N. Xu, L. Peng, Z.X. Zhong, X.M. Fang, P.L. Cen, High-level expression of a soluble functional antimicrobial peptide, human beta-defensin 2, in *Escherichia coli*, Biotechnol. Prog. 22 (2006) 382–386.

[14] Z. Xu, Z.X. Zhong, L. Huang, L. Peng, F. Wang, P. Cen, High-level production of bioactive human beta-defensin-4 in *Escherichia coli* by soluble fusion expression, Appl. Microbiol. Biotechnol. 72 (2006) 471–479.

[15] J.H. Lee, I. Minn, C.B. Park, S.C. Kim, Acidic peptide-mediated expression of the antimicrobial peptide buforin II as tandem repeats in *Escherichia coli*, Protein Expression Purif. 12 (1998) 53–60.

[16] A. Majerle, J. Kidric, R. Jerala, Production of stable isotope enriched antimicrobial peptides in *Escherichia coli*: an application to the production of a N-15-enriched fragment of lactoferrin, J. Biomol. NMR 18 (2000) 145–151.

[17] T.T. Mac, M. Beyermann, J.R. Pires, P. Schmieder, H. Oschkinat, High yield expression and purification of isotopically labelled human endothelin-1 for use in NMR studies, Protein Expression Purif. 48 (2006) 253–260.

[18] F.L. Jin, X.X. Xu, W.Q. Zhang, D.X. Gu, Expression and characterization of a housefly cecropin gene in the methylotrophic yeast, *Pichia pastoris*, Protein Expression Purif. 49 (2006) 39–46.

[19] Q.D. Wei, Y.S. Kim, J.H. Seo, W.S. Jang, I.H. Lee, H.J. Cha, Facilitation of expression and purification of an antimicrobial peptide by fusion with baculoviral polyhedrin in *Escherichia coli*, Appl. Environ. Microbiol. 71 (2005) 5038–5043.

[20] J.Y. Moon, K.A. Henzler-Wildman, A. Ramamoorthy, Expression and purification of a recombinant LL-37 from *Escherichia coli*, Biochim. Biophys. Acta-Biomembr. 1758 (2006) 1351–1358.

[21] X.X. Xu, F.L. Jin, X.Q. Yu, S.X. Ren, J. Hu, W.Q. Zhang, High-level expression of the recombinant hybrid peptide cecropinA(1–8)–magainin2(1–12) with an ubiquitin fusion partner in *Escherichia coli*, Protein Expression Purif. 55 (2007) 175–182.

[22] X.X. Xu, F.L. Jin, X.Q. Yu, S.X. Ji, J. Wang, H.X. Cheng, C. Wang, W.Q. Zhang, Expression and purification of a recombinant antibacterial peptide, cecropin, from *Escherichia coli*, Protein Expression Purif. 53 (2007) 293–301.

[23] S.H. Pyo, J.H. Lee, H.B. Park, J.S. Cho, H.R. Kim, B.H. Han, Y.S. Park, Expression and purification of a recombinant buforin derivative from *Escherichia coli*, Process Biochem. 39 (2004) 1731–1736.

[24] Y. Shen, X.G. Lao, Y. Chen, H.Z. Zhang, X.X. Xu, High-level expression of cecropin X in *Escherichia coli*, Int. J. Mol. Sci. 8 (2007) 478–491.

[25] A.B. Ingham, R.J. Moore, Recombinant production of antimicrobial peptides in heterologous microbial systems, Biotechnol. Appl. Biochem. 47 (2007) 1–9.

[26] B. Japelj, P. Pristovsek, A. Majerle, R. Jerala, Structural origin of endotoxin neutralization and antimicrobial activity of a lactoferrin-based peptide, J. Biol. Chem. 280 (2005) 16955–16961.

[27] R. Jerala, B. Japelj, P. Pristovsek, A. Majerle, Tertiary structure of lactoferrin peptide in complex with LPS for design of novel endotoxin-neutralizing peptides, Shock 21 (2004) 62.

[28] A. Majerle, J. Kidric, R. Jerala, Enhancement of antibacterial and lipopolysaccharide binding activities of a human lactoferrin peptide fragment by the addition of acyl chain, J. Antimicrob. Chemother. 51 (2003) 1159–1165.

[29] N. Papo, Y. Shai, Can we predict biological activity of antimicrobial peptides from their interactions with model phospholipid membranes? Peptides 24 (2003) 1693–1703.

[30] R. Sood, Y. Domanov, P.K.J. Kinnunen, Fluorescent temporin B derivative and its binding to liposomes, J. Fluoresc. 17 (2007) 223–234.

[31] D.I. Chan, E.J. Prenner, H.J. Vogel, Tryptophan- and arginine-rich antimicrobial peptides: structures and mechanisms of action, Biochim. Biophys. Acta 1758 (2006) 1184–1202.

[32] A. Kuliopulos, C.T. Walsh, Production, purification, and cleavage of tandem repeats of recombinant peptides, J. Am. Chem. Soc. 116 (1994) 4599–4607.

[33] P.N. Yadav, Z.H. Liu, M.M. Rafi, A diarylheptanoid from lesser galangal (*Alpinia officinarum*) inhibits proinflammatory mediators via inhibition of mitogen-activated protein kinase, p44/42, and transcription factor nuclear factor-kappa B, J. Pharmacol. Exp. Ther. 305 (2003) 925–931.

[34] S.H. Smallcombe, S.L. Patt, P.A. Keifer, WET solvent suppression and its applications to LC NMR and high-resolution NMR spectroscopy. J. Magn. Reson., Ser. A 117 (2) (1995) 295–303.

[35] M. Piotto, V. Saudek, V. Sklenar, Gradient-tailored excitation for single-quantum NMR spectroscopy of aqueous solutions, 2 (1992) 661.

[36] P. Pristovsek, H. Ruterjans, R. Jerala, Semiautomatic sequence-specific assignment of proteins based on the tertiary structure–the program st2nmr, 23 (2002) 335.

[37] P. Guntert, W. Braun, K. Wuthrich, Efficient computation of three-dimensional protein structures in solution from nuclear magnetic resonance data using the program DIANA and the supporting programs CALIBA, HABAS and GLOMSA, 217 (1991) 517.

[38] R.A. Laskowski, J.A. Rullmannn, M.W. MacArthur, R. Kaptein, J.M. Thornton, AQUA and PROCHECK-NMR: programs for checking the quality of protein structures solved by NMR, 8 (1996) 477.

[39] R. Koradi, M. Billeter, K. Wuthrich, MOLMOL: a program for display and analysis of macromolecular structures, 14 (1996) 51.

[40] D. Piszkiew, M. Landon, E.L. Smith, Anomalous cleavage of aspartyl–proline peptide bonds during amino acid sequence determinations, Biochem. Biophys. Res. Commun. 40 (1970) 1173–1178.

[41] I. Segalas, R. Thai, R. Menez, C. Vita, A particularly labile Asp–Pro bond in the green mamba muscarinic toxin Mtx2 — effect of protein conformation on the rate of cleavage, FEBS Lett. 371 (1995) 171–175.

[42] M.E. Lidell, M.E.V. Johansson, G.C. Hansson, An autocatalytic cleavage in the c terminus of the human MUC2 mucin occurs at the low pH of the late secretory pathway, J. Biol. Chem. 278 (2003) 13944–13951.

[43] E.L. Smith, M. Landon, D. Piszkiew, W.J. Brattin, T.J. Langley, M.D. Melamed, Bovine liver glutamate dehydrogenase — tentative amino acid sequence — Identification of a reactive lysine — nitration of a specific tyrosine and loss of allosteric inhibition by guanosine triphosphate, Proc. Natl. Acad. Sci. U. S. A. 67 (1970) 724–730.

[44] H.N. Hunter, W.G. Jing, D.J. Schibli, T. Trinh, I.Y. Park, S.C. Kim, H.J. Vogel, The interactions of antimicrobial peptides derived from lysozyme with model membrane systems, Biochim. Biophys. Acta-Biomembr. 1668 (2005) 175–189.

[45] R.F. Epand, R.I. Lehrer, A. Waring, W. Wang, R. Maget-Dana, D. Lelievre, R.M. Epand, Direct comparison of membrane interactions of model peptides composed of only Leu and Lys residues, Biopolymers 71 (2003) 2–16.

[46] K. Wüthrich, NMR of Proteins and Nucleic Acids, Wiley & Sons, 1986.

[47] D.S. Wishart, B.D. Sykes, F.M. Richards, Relationship between nuclear magnetic resonance chemical shift and protein secondary structure, J. Mol. Biol. 222 (1991) 311–333.

[48] W. Jing, J.S. Svendsen, H.J. Vogel, Comparison of NMR structures and model-membrane interactions of 15-residue antimicrobial peptides derived from bovine lactoferricin, Biochem. Cell Biol. 84 (2006) 312–326.

[49] C. Haught, G.D. Davis, R. Subramanian, K.W. Jackson, R.G. Harrison, Recombinant production and purification of novel antisense antimicrobial peptide in *Escherichia coli*, Biotechnol. Bioeng. 57 (1998) 55–61.

[50] J.C. Pierce, W.L. Maloy, L. Salvador, C.F. Dungan, Recombinant expression of the antimicrobial peptide polyphemusin and its activity against the protozoan oyster pathogen *Perkinsus marinus*, Mol. Mar. Biol. Biotechnol. 6 (1997) 248–259.

[51] A. Majerle, J. Kidric, R. Jerala, Production of stable isotope enriched antimicrobial peptides in *Escherichia coli*: an application to the production of a 15N-enriched fragment of lactoferrin, J. Biomol. NMR 18 (2000) 145–151.

[52] Y.L. Pan, J.T. Cheng, J. Hale, J. Pan, R.E. Hancock, S.K. Straus, Characterization of the structure and membrane interaction of the antimicrobial peptides aurein 2.2 and 2.3 from Australian southern bell frogs, Biophys. J. 92 (2007) 2854–2864.

[53] L.E. Yandek, A. Pokorny, P.F. Almeida, Small changes in the primary structure of transportan 10 alter the thermodynamics and kinetics of its interaction with phospholipid vesicles, Biochemistry 47 (2008) 3051–3060.

[54] D.J. Schibli, L.T. Nguyen, S.D. Kernaghan, O. Rekdal, H.J. Vogel, Structure–function analysis of tritrpticin analogs: potential relationships between antimicrobial activities, model membrane interactions, and their micelle-bound NMR structures, Biophys. J. 91 (2006) 4413–4426.

[55] A. Tossi, L. Sandri, A. Giangaspero, Amphipathic, alpha-helical antimicrobial peptides, Biopolymers 55 (2000) 4–30.

[56] A. Wessolowski, M. Bienert, M. Dathe, Antimicrobial activity of arginine- and tryptophan-rich hexapeptides: the effects of aromatic clusters, D-amino acid substitution and cyclization, J. Pept. Res. 64 (2004) 159–169.

[57] Z. Liu, A. Brady, A. Young, B. Rasimick, K. Chen, C. Zhou, N.R. Kallenbach, Length effects in antimicrobial peptides of the (RW)n series, Antimicrob. Agents Chemother. 51 (2007) 597–603.

[58] M.B. Strom, B.E. Haug, O. Rekdal, M.L. Skar, W. Stensen, J.S. Svendsen, Important structural features of 15-residue lactoferricin derivatives and methods for improvement of antimicrobial activity, Biochem. Cell Biol. 80 (2002) 65–74.

[59] M. Tang, A.J. Waring, M. Hong, Phosphate-mediated arginine insertion into lipid membranes and pore formation by a cationic membrane peptide from solid-state NMR, J. Am. Chem. Soc. 129 (2007) 11438–11446.

[60] B. Japelj, M. Zorko, A. Majerle, P. Pristovsek, S. Sanchez-Gomez, G. Martinez de Tejada, I. Moriyon, S.E. Blondelle, K. Brandenburg, J. Andra, K. Lohner, R. Jerala, The acyl group as the central element of the structural organization of antimicrobial lipopeptide, J. Am. Chem. Soc. 129 (2007) 1022–1023.

[61] J.A. Mitchell, M.J. Paul-Clark, G.W. Clarke, S.K. McMaster, N. Cartwright, Critical role of toll-like receptors and nucleotide oligomerisation domain in the regulation of health and disease, J. Endocrinol. 193 (2007) 323–330.